Response of a Single Cell to an External Electric Field

Wanda Krassowska* and John C. Neu‡
*Department of Biomedical Engineering and Duke–North Carolina NSF/ERC, Duke University, Durham, North Carolina 27706, and ‡Department of Mathematics, University of California at Berkeley, Berkeley, California USA

ABSTRACT The response of a cell to an external electric field is investigated using dimensional analysis and singular perturbation. The results demonstrate that the response of a cell is a two-stage process consisting of the initial polarization that proceeds with the cellular time constant (<1 μs), and of the actual change of physiological state that proceeds with the membrane time constant (several milliseconds). The second stage is governed by an ordinary differential equation similar to that of a space-clamped membrane patch but formulated in terms of intracellular rather than transmembrane potential. Therefore, it is meaningful to analyze the physiological state and the dynamics of a cell as a whole instead of the physiological states and the dynamics of the underlying membrane patches. This theoretical result is illustrated with an example of an excitation of a cylindrical cell by a transverse electric field.

GLOSSARY

Regions and surfaces

Ω_i, Ω_e	inside and outside regions of the cell
Γ	excitable membrane separating Ω_i and Ω_e
S	area of the cell membrane

Material constants

σ_i, σ_e	specific conductivities of intra- and extracellular regions
μ	extracellular conductivity measured in units of σ_i
R_m, C_m	surface resistance and capacitance of the membrane
d_c	typical dimension of a cell; in a cylindrical cell, diameter
ΔV	amplitude of an action potential
τ_c	cellular time constant equal to $d_c C_m/\sigma_i$
τ_m	membrane time constant equal to $R_m C_m$
τ_{ip}	time constant of initial polarization
ϵ	small, dimensionless parameter, defined as the ratio τ_c/τ_m

Potentials

Φ_i, Φ_e	potentials in intra-, extracellular regions
Φ_m	transmembrane potential
ϕ_i^0, ϕ_e^0	leading order intra-, extracellular potentials
ϕ_m^0	leading order transmembrane potential
v_m^0	transmembrane potential averaged over the cell membrane
V_o	transmembrane potential at the time the field is applied

Fields and currents

$\mathbf{E}$, E	external electric field and its magnitude
I_{ion}	pointwise ionic current of the excitable membrane
i_{ion}	ionic current averaged over the cell membrane

Independent variables and operations

$\mathbf{x}$	position vector
t	time variable
∂_t	derivative with respect to time
$\hat{n}$	unit vector pointing in the direction normal to the membrane
$\mathbf{w}$	vector of weight functions

INTRODUCTION

The response of a single cell to an external electric field has received a significant amount of attention in the literature because of its possible relevance to the mechanism of defibrillation (Plonsey and Barr, 1986; Krassowska et al., 1987; Chernysh et al., 1988; Dillon, 1991). Recent experiments performed on single cells measured the strength of the electric field required to excite isolated ventricular cells (Tung et al., 1991; Bardou et al., 1990) confirmed the existence of the negative and positive transmembrane potential on the opposite ends of a myocyte and investigated the dependence of this potential on the strength of the electric field (Knisley et al., 1993). However, since the transmembrane potential in a single cell is difficult to measure and control, there is virtually no data related to the dynamics of a single cell in an external field.

In the absence of experimental data, the dynamics of a single cell has been extrapolated from the dynamics of a space-clamped membrane patch. For example, the excitation in a membrane patch is preceded by passive depolarization of the membrane with current supplied by the electrodes which proceeds with the time constant on the order of several milliseconds. The excitation occurs when the transmembrane potential exceeds the threshold value. However, the space-clamped membrane is uniformly polarized so that the excitation process is unaffected by the spatial interference from adjacent regions. In contrast, the transmembrane potential of a cell stimulated by an external field varies from positive (depolarized) at the end of a cell facing the cathode to negative (hyperpolarized) at the end facing the anode. To account for this difference, in extrapolating to a single cell, the ex-

Received for publication 25 May 1993 and in final form 7 March 1994.
Address reprint requests to Wanda Krassowska, Department of Biomedical Engineering, Duke University, Durham, NC 27706. Tel.: 919-660-5105; Fax: 919-660-5405.

0006-3495/94/06/1768/09 $2.00

citation process of a membrane has been supplemented with a "loading effect" exerted by the opposite, hyperpolarized end of the cell. Computer simulations of a single, excitable cell in an external field (Tung and Borderies, 1992.; Leon et al., 1993) indicate that such an extrapolation is not entirely correct. For example, the hyperpolarized end of the cell is not a "load" counteracting excitation: its inward flow of potassium current is crucial to the excitation process.

This example shows that the behavior of a single cell in an external electric field is not yet thoroughly understood. While important insights have been provided by numerical studies referenced above, further progress in this area is hampered by the difficulties of obtaining the solution to a single cell problem. The boundary value problem for a fully excitable cell is by no means trivial because of nonlinear boundary conditions on the membrane. The researchers must either drastically simplify the model with accompanying loss of accuracy (Tung and Borderies, 1992; Quan and Cohen, 1993) or engage considerable computing and programming resources (Leon et al., 1993). Furthermore, qualitative understanding gained from a purely numerical analysis is limited. Clearly, more convenient ways of analyzing and solving the single cell problem are needed.

This study demonstrates that the boundary value problem for a single cell reduces at leading order to an ordinary differential equation that governs the dynamics of the cell as a whole. The governing equation is general and applies to cells of any shape as long as their dimensions are short in comparison with the length constant of the tissue, to membrane dynamics described by any model, and to stimulation in any phase of an action potential. Thus, the interaction of a cell with an external field can be studied in a manner similar to that of the membrane patch, cutting down on the computational requirements and allowing the use of nonlinear dynamics methods to gain a qualitative insight in the mechanism of stimulation with the external field. This result was derived using dimensional analysis and the perturbation method. In the past, a similar analysis was performed for a membrane patch and for myelinated and unmyelinated axons by FitzHugh (1973) and for a single cell stimulated by an intracellular source and extracellular sink by Barcilon et al. (Barcilon et al., 1971) and Peskoff et al. (Peskoff and Eisenberg, 1975; Peskoff et al., 1976).

BASIC EQUATIONS AND DIMENSIONAL ANALYSIS

Consider an idealized model of a single cell in an external electric field shown in Fig. 1. Intra- and extracellular regions are assumed purely resistive, with conductivities σ_i and σ_e. Hence, intra- and extracellular potentials satisfy Laplace's equations,

$$\begin{aligned} \nabla^2\Phi_i &= 0 \quad \text{in} \quad \Omega_i \\ \nabla^2\Phi_e &= 0 \quad \text{in} \quad \Omega_e. \end{aligned} \tag{1}$$

The boundary conditions on the external surface $\partial\Omega_e$ are

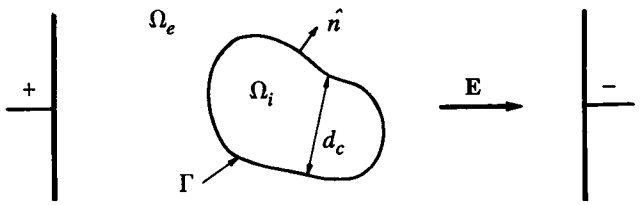

FIGURE 1 Idealized representation of a single cell in an external electric field. An excitable membrane is represented by a closed surface Γ that separates the interior of the cell Ω_i from the surrounding medium Ω_e. The intracellular region Ω_i has a typical dimension d_c, usually on the order of micrometers. Electric field **E** is established by a pair of external electrodes and is assumed uniform in the vicinity of the cell.

determined by the experimental setup. However, if the cell is small compared with the extracellular region, and if it is located away from the electrodes, the electric field is approximately uniform in the vicinity of the cell. Therefore, the details of the experimental setup can be neglected. In such a case, the extracellular potential far away from the cell corresponds to the uniform electric field

$$\Phi_e(\mathbf{x}, t) = -\mathbf{E} \cdot \mathbf{x} \qquad \text{as} \quad |\mathbf{x}| \to \infty. \tag{2}$$

On the membrane Γ, the potential is discontinuous, and the difference between intra- and extracellular potentials is the transmembrane potential $\Phi_m(t)$

$$\Phi_m = \Phi_i - \Phi_e \qquad \text{on} \quad \Gamma. \tag{3}$$

The current through the membrane is continuous. Normal current densities in both regions are equal to the membrane current per unit area which consists of capacitive and ionic components

$$\begin{aligned} -\hat{n} \cdot \{\sigma_i \nabla\Phi_i\} &= C_m \partial_t \Phi_m + I_{ion}(\Phi_m) \\ -\hat{n} \cdot \{\sigma_e \nabla\Phi_e\} &= C_m \partial_t \Phi_m + I_{ion}(\Phi_m) \end{aligned} \qquad \text{on} \quad \Gamma, \tag{4}$$

where $\hat{n}$ is a unit normal pointing outward from the cell, ∂_t denotes the derivative with respect to time, and C_m is the surface capacitance of the membrane. The ionic current I_{ion} is determined by a complex dynamics of the excitable membrane and consists of several nonlinear dynamic currents carried by different ions. For the purpose of this study, these details are not important: the excitability of the membrane will be represented by the total ionic current I_{ion} viewed as depending on the transmembrane potential Φ_m (Fig. 2). To simplify presentation, Fig. 2 assumes that the rest state occurs at the zero membrane potential, ignoring a constant of about −85 mV. Consequently, potentials Φ_m, Φ_i, and Φ_e should be understood as deviations from their rest values.

Solutions to the single cell problem (Eqs. 1–4) are determined up to an arbitrary function of time added to both Φ_i and Φ_e. To obtain a unique solution, Eqs. 1–4 must be supplemented by a normalization condition. It is convenient to assume it in the form

$$\int_\Gamma \Phi_e \, da = 0. \tag{5}$$

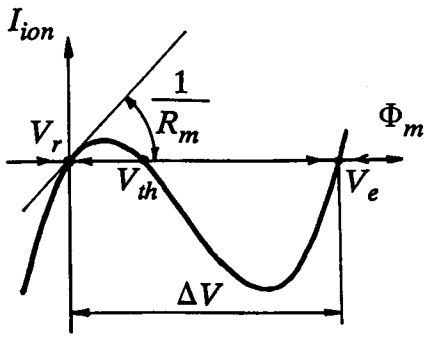

FIGURE 2 An example of the current-voltage relationship of an excitable membrane. The N-shaped relationship between transmembrane potential Φ_m and ionic current I_{ion} is typical for short intervals after the application of the stimulus (compare Fig. 13 of the paper by Hodgkin et al., 1952). It has three intersection points with the horizontal axis representing three physiological states of the membrane. Two of these states, the rest state $\Phi_m = V_r$ and the excited state $\Phi_m = V_e$, are stable. The third state, $\Phi_m = V_{th}$, is unstable and corresponds to the threshold phenomenon. The figure defines two fundamental constants related to the excitable membrane: ΔV, the amplitude of the action potential, and R_m, the surface resistance of the membrane measured at rest.

Eqs. 1–5 can be converted into nondimensional form with the following system of units:

potentials:	ΔV, amplitude of action potential;
conductivities:	σ_i, intracellular conductivity;
membrane currents:	$\Delta V/R_m$;
distance:	d_c, typical cell dimension;
electric fields:	$\Delta V/d_c$;
time:	$\tau_c = d_c C_m/\sigma_i$, cellular time constant; and $\tau_m = R_m C_m$, membrane time constant.

The presence of two time scales, τ_c and τ_m, indicates that a single cell responds to an external field in two stages. The first stage takes place immediately after the external field is turned on and describes charging the cell membrane with intra- and extracellular currents. This stage is called "initial polarization" of the cell. The second stage describes the actual change of the physiological state of the cell caused by the field. For example, during excitation, the second stage describes the process that takes cell from the rest state to the excited state. In the language of singular perturbation theory, initial polarization that proceeds with a cellular time constant τ_c (<1 μs) constitutes an initial layer of the second stage that proceeds with a much longer membrane time constant τ_m (several milliseconds) (Bender and Orszag, 1978).

INITIAL POLARIZATION

The problem describing initial polarization is obtained by scaling Eqs. 1–5 with the system of units given above and with a cellular time constant τ_c as a unit of time. Laplace's equations (Eq. 1), boundary conditions (Eqs. 2 and 3), and the normalization condition (Eq. 5) remain unchanged; the nondimensional boundary conditions on currents are:

$$\begin{aligned} -\hat{n}\cdot\nabla\Phi_i &= \partial_t\Phi_m + \epsilon I_{ion}(\Phi_m) \\ -\mu\hat{n}\cdot\nabla\Phi_e &= \partial_t\Phi_m + \epsilon I_{ion}(\Phi_m) \end{aligned} \quad \text{on} \quad \Gamma. \tag{6}$$

Here, $\mu = \sigma_e/\sigma_i$, I_{ion} is a nondimensional ionic current, and ϵ is a small, dimensionless parameter formed from fundamental material constants

$$\epsilon = \frac{d_c}{R_m\sigma_i}, \tag{7}$$

that has a typical magnitude of $6.25 \cdot 10^{-3}$. In the boundary conditions (Eq. 6), ϵ multiplies I_{ion} indicating that during initial polarization, the ionic current is orders of magnitude smaller than the capacitive current. Indeed, if solutions to Eqs. 1–3 and 6 are sought as expansions in powers of ϵ,

$$\begin{aligned} \Phi_i(\mathbf{x}, t, \epsilon) &= \phi_i^0 + \epsilon\phi_i^1 + \cdots && \text{in} \quad \Omega_i \\ \Phi_e(\mathbf{x}, t, \epsilon) &= \phi_e^0 + \epsilon\phi_e^1 + \cdots && \text{in} \quad \Omega_e \\ \Phi_m(\mathbf{x}, t, \epsilon) &= \phi_m^0 + \epsilon\phi_m^1 + \cdots && \text{on} \quad \Gamma, \end{aligned} \tag{8}$$

then in the limit $\epsilon \to 0$, the leading order potentials ϕ_i^0, ϕ_e^0, and ϕ_m^0 satisfy Laplace's equations with the following boundary conditions:

$$\begin{aligned} -\hat{n}\cdot\nabla\phi_i^0 &= \partial_t\phi_m^0 \\ -\mu\hat{n}\cdot\nabla\phi_e^0 &= \partial_t\phi_m^0 \end{aligned} \quad \text{on} \quad \Gamma. \tag{9}$$

Eq. 9 contains no ionic current, and hence the membrane during initial polarization behaves as a pure capacitance.

The initial polarization problem requires initial conditions on potentials at time $t = 0^+$. These are determined, in general, by solving a boundary value problem determined by Eqs. 1–3, subject to the following boundary conditions on the membrane:

$$\begin{aligned} -\hat{n}\cdot\nabla\phi_i^0 &= -\mu\hat{n}\cdot\nabla\phi_e^0 \\ \phi_m^0(\mathbf{x}, 0^+) &= V_o. \end{aligned} \tag{10}$$

At $t = 0^+$, the current across the membrane is continuous and the transmembrane potential remains unchanged because the finite external current cannot instantaneously change the charge on the membrane capacitance. The value V_o depends on the physiological state of the membrane at the time the field is applied and is independent of the position on the membrane.

For simple geometries, the initial polarization problem described by Eqs. 1–3, 9, and 10 can be readily solved. The solution for a cylindrical cell is given in the section on excitation of a cylindrical cell. Solutions for cells of other geometries, both steady-state (Klee, 1973; Klee and Plonsey, 1976; Irnich, 1990) and time-dependent (Teissie and Tsong, 1981; Schwann, 1983; Cartee and Plonsey, 1992), can be found in the literature.

Of particular interest are the steady-state solutions because they serve as initial conditions to the problem governing the subsequent evolution of potentials that proceeds with the

time constant τ_m. For a cell of an arbitrary shape, intra- and extracellular potentials at the end of the initial polarization are determined by the following boundary value problems. In the extracellular space,

$$\begin{aligned} \nabla^2\phi_e^0 &= 0 && \text{in} \quad \Omega_e \\ \hat{n}\cdot\nabla\phi_e^0 &= 0 && \text{on} \quad \Gamma \\ \phi_e^0(\mathbf{x}) &= -\mathbf{E}\cdot\mathbf{x} && \text{as} \quad |\mathbf{x}|\to\infty \\ \int_\Gamma \phi_e^0\, da &= 0. \end{aligned} \tag{11}$$

Problem 11 has a linear dependence on the electric field $\mathbf{E}$. Thus, extracellular potential is sought in the form

$$\phi_e^0(\mathbf{x}, \mathbf{E}) = \mathbf{E}\cdot\mathbf{w}(\mathbf{x}), \tag{12}$$

where $\mathbf{w}$ is a vector of weight functions. Computing w_i involves solving Eq. 11 with ith component of electric field $\mathbf{E}$ set to 1 and other components to 0. In the intracellular space,

$$\begin{aligned} \nabla^2\phi_i^0 &= 0 && \text{in} \quad \Omega_i \\ \hat{n}\cdot\nabla\phi_i^0 &= 0 && \text{on} \quad \Gamma. \end{aligned} \tag{13}$$

Eq. 13 implies that the leading order intracellular potential will be constant throughout the interior of the cell. The normalization condition (Eq. 5) together with boundary conditions (Eq. 9) and the initial condition on transmembrane potential (Eq. 10) imply that

$$\phi_i^0 = V_o, \tag{14}$$

i.e., the intracellular potential is determined by the state of the cell at the time the field was applied. Consequently, the leading order transmembrane potential has the form

$$\phi_m^0(\mathbf{x}, \mathbf{E}) = V_o - \mathbf{E}\cdot\mathbf{w}(\mathbf{x}) \tag{15}$$

evaluated for $\mathbf{x}$ belonging to Γ. Hence, the transmembrane potential varies with the position around the cell: ϕ_m^0 is the smallest at the end of the cell facing the anode and the largest at the opposite end.

CHANGE IN THE PHYSIOLOGICAL STATE

Further time evolution of these potentials and, in particular, the possibility of changes in the physiological state of the cell membrane, depend on the ionic current I_{ion}. The initial polarization cannot determine whether such changes occur because the ionic current in Eq. 9 has been eliminated by scaling. Hence, to answer this question, one must examine the long time behavior of the cell. The problem governing the active response is obtained by scaling Eqs. 1–5 with units given in the section on basic equations and dimensional analysis and with τ_m as a unit of time. Laplace's equations (Eq. 1), boundary conditions (Eqs. 2 and 3), and the normalization condition (Eq. 5) remain unchanged; the nondimensional boundary conditions on currents are:

$$-\hat{n}\cdot\nabla\Phi_i = \epsilon\{\partial_t\Phi_m + I_{ion}(\Phi_m)\} \tag{16.1}$$

$$-\mu\hat{n}\cdot\nabla\Phi_e = \epsilon\{\partial_t\Phi_m + I_{ion}(\Phi_m)\} \quad \text{on} \quad \Gamma. \tag{16.2}$$

Note that in this problem, all currents flowing through the membrane, i.e., both capacitive and ionic components, are multiplied by a small parameter ϵ. Hence, in a leading order approximation, the membrane behaves as an insulator. That is precisely the situation that developed at the end of the initial polarization; consequently, the steady-state solutions of the initial polarization serve as initial conditions to the problem describing the active response of the cell.

Solutions to this problem can be obtained numerically by discretizing (Eqs. 1–3 and 16) and solving them on a computer. In essence, the cell will be treated as a collection of membrane patches and the physiological states of those patches will determine the physiological state of the whole cell. An alternative approach is to recognize that the boundary value problem (Eqs. 1–3 and 16) reduces at leading order to an ordinary differential equation that governs the response of a cell treated as a whole. To show this, one must examine the macroscopic balance of current. The net current entering or leaving the cell is computed by integrating Eq. 16.1 over the membrane Γ. The integral of the intracellular current (left hand side) is zero because the cell is source-free. Hence, the net capacitive current entering or leaving the cell is balanced by the net ionic current

$$\int_\Gamma \partial_t\Phi_m\, da = -\int_\Gamma I_{ion}(\Phi_m)\, da. \tag{17}$$

Eq. 17 indicates that during the actual change of the physiological state, the cell has no net exchange of current with the environment. The active response of the cell draws upon the charge stored in the membrane during initial polarization.

Integral identity (Eq. 17) can be approximated by an ordinary differential equation. First, recognize that in a limit $\epsilon \to 0$, Eqs. 1–3 and 16 have no time dependence. Thus, the leading order potentials will retain the same form established by the initial polarization except for a time-dependent constant. As shown in the previous section, intracellular potential is constant throughout the interior of the cell; this constant may subsequently evolve with time. Extracellular potential is given by $\mathbf{E}\cdot\mathbf{w}$ and does not depend on time. This result is motivated physically: a small net ionic current crossing the membrane can easily change potential inside a cell that is only several micrometers in diameter. However, the same current has practically no impact on the extracellular potential, because the extracellular region Ω_e is large and because the extracellular field is enforced by the electrodes. Thus, in the limit $\epsilon \to 0$, the leading order intracellular potential depends only on time t, while the leading order extracellular potential depends on the position $\mathbf{x}$ and, parametrically, on the electric field $\mathbf{E}$:

$$\begin{aligned} \Phi_i(\mathbf{x}, t, 0) &= \phi_i^0(t) \\ \Phi_e(\mathbf{x}, t, 0) &= \phi_e^0(\mathbf{x}, \mathbf{E}) = \mathbf{E}\cdot\mathbf{w}(\mathbf{x}). \end{aligned} \tag{18}$$

Second, define the macroscopic ionic current i_{ion} as an average of the pointwise ionic current I_{ion} over the surface of the membrane S,

$$i_{ion}(\phi_i^0, \mathbf{E}) = \frac{1}{S}\int_\Gamma I_{ion}(\phi_m^0)\,da = \frac{1}{S}\int_\Gamma I_{ion}(\phi_i^0 - \mathbf{E}\cdot\mathbf{w})\,da. \tag{19}$$

For a given geometry of a cell and the dynamics of the membrane, this macroscopic ionic current is a function of intracellular potential ϕ_i^0 and depends parametrically on the field $\mathbf{E}$. Introducing Eqs. 18 and 19 allows writing the macroscopic balance of current (Eq. 17) as

$$\partial_t \phi_i^0 = -i_{ion}(\phi_i^0, \mathbf{E}), \tag{20}$$

or, in the dimensional variables,

$$C_m \partial_t \phi_i^0 = -i_{ion}(\phi_i^0, \mathbf{E}). \tag{21}$$

Equation 21 demonstrates that the active response of a cell to an electric field is governed by an ordinary differential equation. In comparison, the equation governing the response of a space-clamped membrane patch is

$$C_m \partial_t \Phi_m = -I_{ion}(\Phi_m) + \sigma_e E. \tag{22}$$

Equation 22 assumes that the membrane patch is placed in a uniform electric field whose strength E is measured or controlled in the extracellular space; thus, $\sigma_e E$ denotes the stimulating current.

Comparing Eqs. 21 and 22 demonstrates that the behavior of a single cell resembles the behavior of a membrane patch provided that the parallels are drawn between the intracellular potential ϕ_i^0 and the membrane potential Φ_m. The similar form of Eqs. 21 and 22 indicates that a single cell in an external electric field can be treated as a unit. Just as a membrane patch has distinct physiological states associated with the transmembrane potential Φ_m, a single cell can be considered to have its own physiological states, defined in terms of intracellular potential ϕ_i^0. The difference is that in a single cell, the driving force for the time evolution of ϕ_i^0 and, subsequently, for the change of the physiological state is the macroscopic ionic current entering the cell. In contrast, in the membrane, the ionic current opposes the depolarizing influence of the external field.

EXAMPLE: EXCITATION OF A CYLINDRICAL CELL

The theoretical results presented above are illustrated with an example of a cylindrical cell placed in an electric field transverse to its axis and activated during diastole. Here, d_c is the cell diameter, 15 μm, the conductivities are σ_i = 20 mS/cm and σ_e = 4 mS/cm, and the membrane capacitance is C_m = 1 μF/cm^2. The dynamics of the cell membrane is described by the Beeler-Reuter model (Beeler and Reuter, 1977). With these assumptions, the cellular time constant τ_c is 0.4 μs and the membrane time constant τ_m is 6 ms.

The first stage of an excitation process is the initial polarization governed by Eqs. 1–3, 9, and 10. In this example, the cell is assumed to be initially at rest, so V_o, the transmembrane potential prior to the application of the field, is equal to V_r = 0. For a cylindrical cell in a transverse field, the solutions to Eqs. 1–3, 9, and 10 are obtained by separation of variables (Dixon, 1971) and express potentials in cylindrical coordinates as functions of radius r, angle θ, and time t. In dimensional variables, these solutions are:

$$\phi_i^0(r, \theta, t) = -\frac{2\sigma_e}{\sigma_i + \sigma_e} Er\cos\theta\, e^{-t/\tau_{ip}}, \qquad r \le \frac{d_c}{2} \tag{23}$$

$$\phi_e^0(r, \theta, t) = -Er\cos\theta\left[1 + \frac{d_c^2}{4r^2}\left(1 - \frac{2\sigma_i}{\sigma_i + \sigma_e} e^{-t/\tau_{ip}}\right)\right], \qquad r \ge \frac{d_c}{2}$$

$$\phi_m^0(\theta, t) = E\, d_c \cos\theta(1 - e^{-t/\tau_{ip}}), \qquad r = d_c/2.$$

All three potentials evolve with a time constant of initial polarization,

$$\tau_{ip} = \frac{1}{2} d_c C_m \left(\frac{1}{\sigma_i} + \frac{1}{\sigma_e}\right). \tag{24}$$

If intra- and extracellular conductivities were equal, initial polarization would have proceeded with the cellular time constant τ_c = 0.4 μs. For conductivities assumed in this example, τ_{ip} is shorter than τ_c, about 0.24 μs.

The behavior of intra- and extracellular potentials is illustrated in Fig. 3. Immediately after the field is turned on (*dashed lines*), intracellular potential ϕ_i^0 changes linearly with the distance and has the slope higher than the strength of the external field. This is because the intracellular conductivity σ_i is assumed to be five times larger than the extracellular conductivity σ_e. On the membrane Γ, the potential at time 0^+ is continuous, so initially transmembrane potential ϕ_m^0 is 0. Extracellular potential ϕ_e^0 asymptotes with the distance to the straight line corresponding to the applied electric field.

If intra- and extracellular conductivities were equal, the electric fields at $t = 0^+$ would have been equal to E in both intra- and extracellular space. The cell would be totally invisible to the field. With intracellular conductivity higher that extracellular, the field "sees" the interior of the cell, but does not "see" the membrane.

As time increases, the gradient of intracellular potential decreases in magnitude, and ϕ_i^0 asymptotes to a constant value, shown by a solid line. In contrast, the magnitude of the extracellular potential in the proximity of the cell slightly increases in time. At steady state, the slope of ϕ_e^0 at the membrane Γ is 0; that indicates that after initial polarization is complete, the membrane is fully charged and behaves as an insulator: it admits no further current from the environment.

As intracellular and extracellular potentials evolve in time, they lose continuity on the membrane Γ, and the transmembrane potential ϕ_m^0 develops. Fig. 3 *c* shows ϕ_m^0 increasing

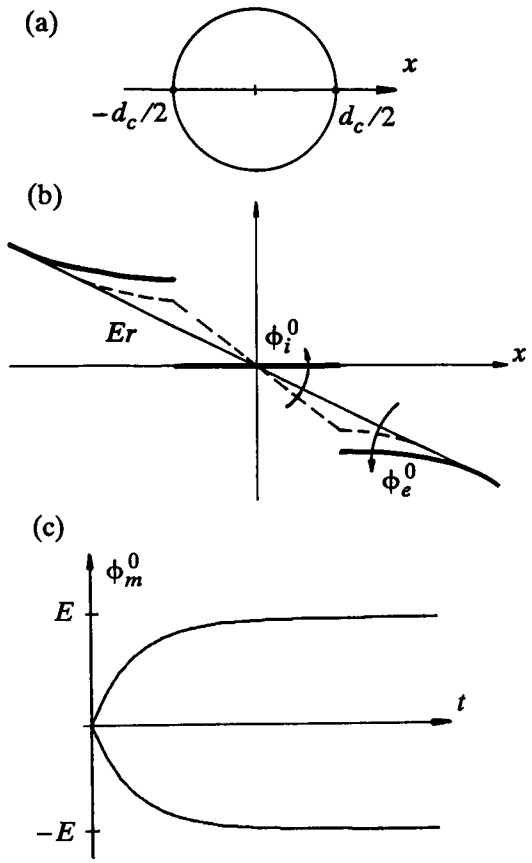

FIGURE 3 Intracellular, extracellular, and transmembrane potentials during initial polarization. The potentials are plotted along axis x connecting two poles of the cell as shown in a. In b, the part of the graph between $-d_c/2$ and $d_c/2$ corresponds to intracellular potential ϕ_i^0, and the part beyond this range corresponds to extracellular potential ϕ_e^0. Dashed lines show intra- and extracellular potentials immediately after the electric field was turned on ($t = 0^+$). As time increases, intra- and extracellular potentials move in the directions indicated by the arrows until they reach the steady state shown by solid lines. A thin line marked $-Er$ is the potential corresponding to the uniform external field. (c) Time course of the transmembrane potential, which increases in time at the end of the cell facing the cathode and decreases at the opposite end.

in time to the steady state value of $E\,d_c$ at the end of the cell facing the cathode and to $-E\,d_c$ at the end facing the anode. After the initial polarization is complete, the final values of potentials are:

$$\phi_i^0(r, \theta) = 0, \qquad r \le d_c/2$$

$$\phi_e^0(r, \theta) = -Er\cos\theta\left(1 + \frac{d_c^2}{4r^2}\right), \qquad r \ge \frac{d_c}{2} \tag{25}$$

$$\phi_m^0(\theta) = E\,d_c\cos\theta, \qquad r = d_c/2.$$

Further time course of these potentials is determined by the second stage of the excitation process which describes the actual transition from the rest to the excited state. The time evolution of this transition is computed from Eq. 21. Alongside, the figures show the excitation of a membrane patch, computed from Eq. 22, to underscore the similarities and differences between the behavior of a single cell and a membrane patch.

Qualitatively, the excitation of a single cell can be analyzed by plotting the time derivative $\partial_t \phi_i^0$ as a function of ϕ_i^0 (Fig. 4 a). From Eq. 21, $\partial_t \phi_i^0$ for a cylindrical cell can be evaluated as

$$\begin{aligned}\partial_t\phi_i^0 &= -\frac{1}{C_m} i_{ion}(\phi_i^0, \mathbf{E}) \\ &= -\frac{1}{2\pi C_m}\int_0^{2\pi} I_{ion}(\phi_i^0 + Ed_c\cos\theta)\,d\theta.\end{aligned} \tag{26}$$

In this example, the cell initially is at rest, so $\phi_i^0 = V_r = 0$. The increase of ϕ_i^0 toward the excited state V_e is initiated by applying an electric field E that raises $\partial_t \phi_i^0$ high enough for the rest state V_r and the threshold V_{th} to coalesce and disappear. With $\partial_t \phi_i^0$ positive in the vicinity of the rest state and to its right, the intracellular potential is forced to increase. After ϕ_i^0 passes the threshold value V_{th}, the excitation continues even if the external field is terminated. The value of the transmembrane potential is not relevant: ϕ_m^0 changes with the position on the membrane and with the strength of the electric field.

The above analysis, conducted for a single cell, resembles that of a membrane patch (Fig. 4 b). The main difference is that b contains the transmembrane potential Φ_m and its time derivative, while a contains intracellular potential ϕ_i^0 and its time derivative. In addition, for the membrane patch, electric field E merely moves $\partial_t \Phi_m$ up or down; in a cell, E not only raises $\partial_t \phi_i^0$ but also changes its shape. Finally, for the membrane patch, a positive electric field raised $\partial_t \Phi_m$ while a negative field lowered it; in a cell, an electric field raises $\partial_t \phi_i^0$ independent of the polarity. Thus, the excitation of a single cell can be achieved with either direction of the external field.

Figs. 5 and 6 use the realistic membrane dynamics (Beeler and Reuter, 1977) to facilitate quantitative comparison between a single cell and a membrane patch. Numerical solutions for these figures were obtained by integrating equations Eqs. 21 and 22 using the Euler method with a time step of 1 μs. The macroscopic ionic current was computed by dividing the circumference of the cell into 64 equipotential patches, computing ionic current I_{ion} for each patch, and

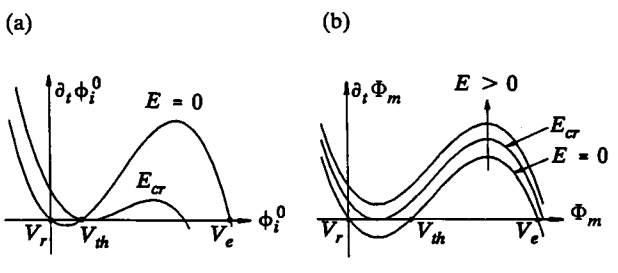

FIGURE 4 Mechanism of excitation of a single cell (a) and a membrane patch (b). In a, the time derivative of the intracellular potential $\partial_t \phi_i^0$ is plotted as a function of ϕ_i^0. In b, the time derivative of the transmembrane potential $\partial_t \Phi_m$ is plotted as a function of Φ_m. For the electric field $E = 0$, both curves are similar to the current-voltage relationship of Fig. 2. E_{cr} denotes the smallest external field required for excitation.

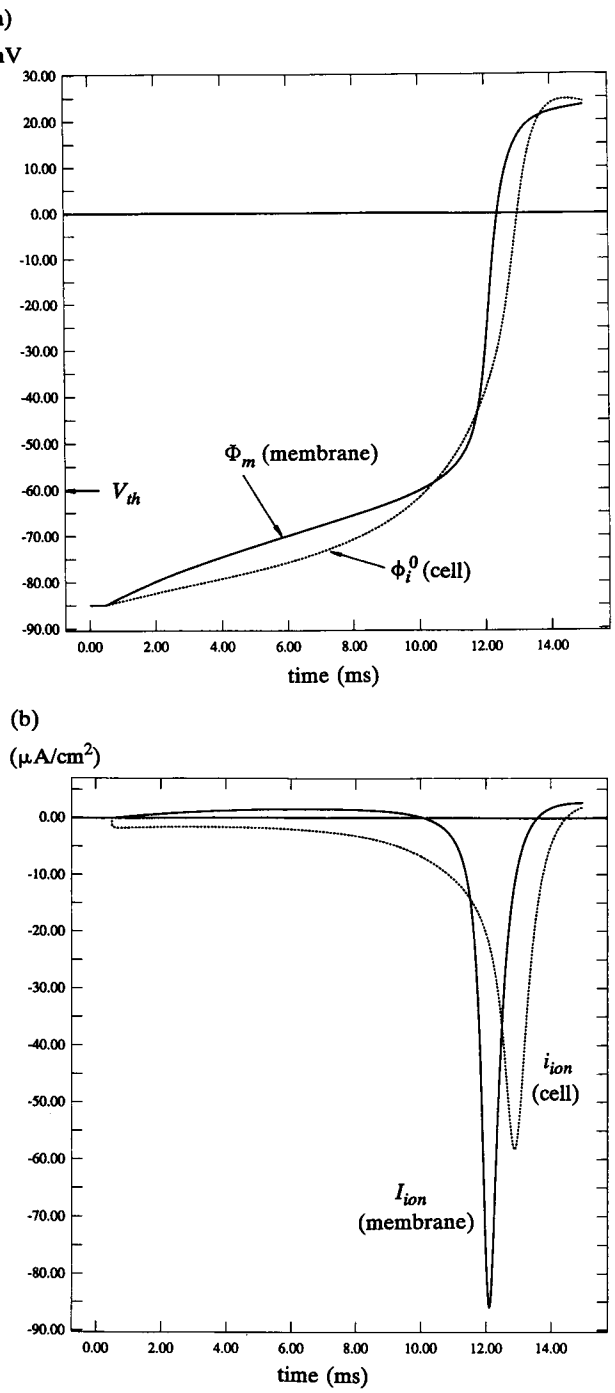

FIGURE 5 The time course of excitation in a single cell and in a membrane patch. (*a*) Intracellular potential ϕ_i^0 for the single cell and the transmembrane potential Φ_m for the membrane patch. (*b*) Macroscopic ionic current i_{ion} for the single cell and the pointwise ionic current I_{ion} for the membrane patch.

using the trapezoidal rule to evaluate the integral. The electric fields were $0.18 \cdot 10^{-3}$ and 16 V/cm for the membrane patch and single cell, respectively, and were kept on for the entire duration of the simulation.

As expected on the basis of qualitative analysis of Fig. 4, the time courses of ϕ_i^0 and Φ_m are very similar. At time $t = 0$, the external field is turned on raising $\partial_t \phi_i^0$ (respectively, $\partial_t \Phi_m$) above the horizontal axis so that the rest state and threshold disappear. However, these phenomena are not immediately reflected in the ϕ_i^0 (Φ_m) since at $t = 0^+$, both remain at rest state V_r. The first feature on the graph is a slow increase of ϕ_i^0 (Φ_m). In a single cell, this increase is due to the macroscopic current i_{ion} flowing inward (Fig. 5 *b, dashed line*). In a membrane patch, the increase is due to charging of the membrane by the external current $\sigma_e E$. The ionic current I_{ion} (Fig. 5 *b, solid line*) flows outward and opposes the depolarizing influence of the external current.

The mechanism behind the increase of ϕ_i^0 is illustrated in Fig. 6. The electric field is turned on and, at time $t = 0^+$, the initial polarization is completed. (Recall that now t is measured on the scale of milliseconds, not microseconds.) This is immediately reflected by the pointwise transmembrane potentials ϕ_m^0 that jump to their maximum values (Fig. 6 *a*), even though the intracellular potential ϕ_i^0 remains at rest (Fig. 5 *a*). The inward macroscopic ionic current (Fig. 5 *b*) initially comes only from the hyperpolarized end of the cell (Fig. 6 *b, curves 3* and *4*, Fig. 6 *c, curve* 0^+). Thus, at time $t = 0^+$ the hyperpolarized end of the cell is not a "load" counteracting excitation. On the contrary, the current entering through the hyperpolarized end is instrumental in initiating the movement of ϕ_i^0 toward the excited state, and it is the depolarized part of the membrane that acts as a "load" (Fig. 6 *c, curve* 0^+).

Soon after the onset of the stimulus, the current in the part of the cell membrane that is depolarized above V_{th} switches inward and assists excitation (Fig. 6 *b, curve 0*). However, the current in the parts of the membrane that is depolarized between V_r and V_{th} remains outward and opposes excitation. This can be seen in Fig. 6 *c*, which shows the distribution of the ionic current around the circumference of the cell. Ten ms after the onset of the stimulus (Fig. 6 *c, curve 10*), the current in the right, depolarized half of the cell has changed inward. At the same time, the left, initially hyperpolarized half has been raised above V_r, and the current has switched outward, becoming a "load" counteracting excitation. However, by this time the success of the excitation is sealed: ϕ_i^0 is above V_{th}, and its further rapid increase quickly raises the transmembrane potential of the entire membrane above threshold.

CONCLUSION

The theory and computer simulations presented here suggest that the cell responds to an external electric field as a unit and does not have to be viewed as a collection of separate membrane patches. The dynamics of a cell as a whole is governed by a first order ordinary differential equation similar to that of a space-clamped membrane, but formulated in terms of the intracellular potential ϕ_i^0 rather than the transmembrane potential. This result greatly simplifies computer simulations which, to date, required solving a boundary value problem with nonlinear boundary conditions. Furthermore, the methods of nonlinear dynamics can now be applied to the problem

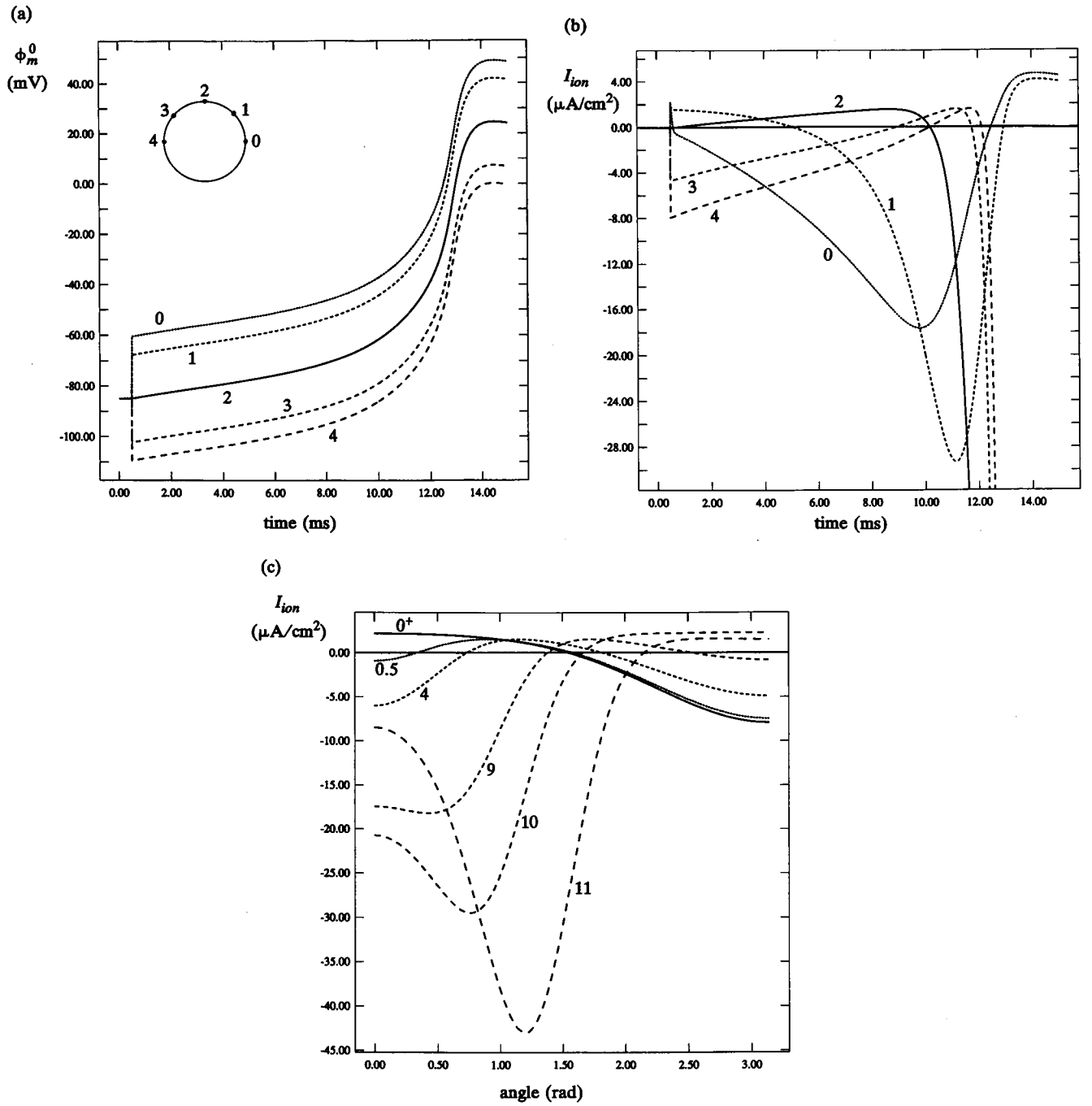

FIGURE 6 Transmembrane potential (*a*) and ionic current (*b*) plotted as a function of time for five points around the circumference of the cell (*a, inset*). After initial polarization, point 0 has maximum depolarization and point 4 has maximum hyperpolarization. (*c*) Ionic current plotted as a function of the position along the circumference of the cell, with 0 corresponding to point 0 and π corresponding to point 4. The six curves correspond to different times after application of the stimulus: 0^+, 0.5, 4, 9, 10, and 11 ms.

leading to qualitative insight into the basic mechanism of the interaction of a single cell with the external electric field.

The computer simulations confirm that during excitation the time evolution of ϕ_i^0 in a cell in many ways parallels the time evolution of Φ_m in a membrane: both start from the rest value V_r and both increase with the same time constant. Excitation is assured when the respective state variable crosses the threshold value V_{th}. The difference is in the driving force that causes Φ_m and ϕ_i^0 to increase: for the membrane patch, it is the competition between the inward, depolarizing current maintained by an external field and the outward, counteracting ionic current. For a single cell, it is the inward, macroscopic ionic current that draws upon the charge stored in the membrane during initial polarization. Hence, the dynamics of excitation in both cases are similar but not identical. These similarities and differences between a membrane

patch and a single cell hold true for a cell of any shape, for any membrane dynamics, and not only for excitation but also for the prolongation of action potential and for any other active response caused by an external field.

Finally, the results of this study offer an interpretation of the measurements of transmembrane potential made with fluorescent dyes (Dillon, 1991). Notice that the normalization condition (Eq. 5) implies that the intracellular potential ϕ_i^0 is equal to the average transmembrane potential, defined as

$$v_m^0(t) = \frac{1}{S}\int_\Gamma \phi_m^0(\mathbf{x}, t)\, da. \tag{27}$$

With Eq. 27, the macroscopic ionic current (Eq. 19), and, consequently, the time evolution equation governing the active response of a cell (Eq. 21) can be expressed also in terms of the average transmembrane potential v_m^0,

$$C_m \partial_t v_m^0 = -i_{ion}(v_m^0, \mathbf{E}). \tag{28}$$

Comparing Eqs. 21 and 28 demonstrates that either intracellular potential ϕ_i^0 or averaged transmembrane potential v_m^0 can act as a state variable. The choice is arbitrary. This paper uses ϕ_i^0 as a state variable because ϕ_i^0 is a real, physically existing potential that can be directly measured with a microelectrode. However, v_m^0 can also be measured, although only indirectly, through optical signals from fluorescent dyes which are considered proportional to the spatially averaged transmembrane potential. Since either quantity, ϕ_i^0 and v_m^0, is a legitimate state variable for the whole cell, the optical signal should be interpreted as reflecting the macroscopic dynamics of the tissue.

This work was supported in part by National Science Foundation Engineering Research Center Grant CDR-8622201.

REFERENCES

Barcilon, V., J. D. Cole, and R. S. Eisenberg. 1971. A singular perturbation analysis of induced electric fields in nerve cells. *SIAM J. Appl. Math.* 21:339–354.

Bardou, A. L., J-M. Chesnais, P. J. Birkui, M-C. Govaere, P. M. Auger, D. Von Euw, and J. Degonde. 1990. Directional variability of stimulation threshold measurements in isolated guinea pig cardiomyocytes: relationship with orthogonal sequential defibrillating pulses. *PACE.* 13: 1590–1595.

Beeler, G. W., and H. Reuter. 1977. Reconstruction of the action potential of ventricular myocardial fibres. *J. Physiol.* 268:177–210.

Bender, C. M., and S. Orszag. 1978. Advanced Mathematical Methods for Scientists and Engineers. McGraw-Hill, New York.

Cartee, L. A., and R. Plonsey. 1992. The transient subthreshold response of spherical and cylindrical cell models to extracellular stimulation. *IEEE Trans. Biomed. Eng.* 39:76–85.

Chernysh, A. M., V. Y. Tabak, and M. S. Bogushevich. 1988. Mechanisms of electrical defibrillation of the heart. *Resuscitation.* 16:169–178.

Dillon, S. M. 1991. Optical recordings in the rabbit heart show that defibrillation strength shocks prolong the duration of depolarization and the refractory period. *Circ. Res.* 69:842–856.

Dixon, C. 1971. Applied Mathematics of Science and Engineering. John Wiley & Sons, New York.

FitzHugh, R. 1973. Dimensional analysis of nerve models. *J. Theor. Biol.* 40:517–541.

Hodgkin, A. L., A. F. Huxley, and B. Katz. 1952. Measurement of current-voltage relations in the membrane of the giant axon of *Loligo. J. Physiol.* 116:424–448.

Irnich, W. 1990. The fundamental law of electrostimulation and its application to defibrillation. *PACE.* 13:1433–1447.

Klee, M. 1973. Intracellular biopotentials during static extracellular stimulation. *Biophys. J.* 13:822–831.

Klee, M., and R. Plonsey. 1976. Stimulation of spheroidal cells: the role of cell shape. *IEEE Trans. Biomed. Eng.* 23:347–354.

Knisley, S. B., T. F. Blitchington, B. C. Hill, A. O. Grant, W. M. Smith, T. C. Pilkington, and R. E. Ideker. 1993. Optical measurements of transmembrane potential changes during electric field stimulation of ventricular cells. *Circ. Res.* 72:255–270.

Krassowska, W., T. C. Pilkington, and R. E. Ideker. 1987. Periodic conductivity as a mechanism for cardiac stimulation and defibrillation. *IEEE Trans. Biomed. Eng.* 34:555–560.

Leon, L. J., H. Hogues, and F. A. Roberge. 1993. A model study of extracellular stimulation of cardiac cells. *IEEE Trans. Biomed. Eng.* 40: 1307–1319.

Peskoff, A., and R. S. Eisenberg. 1975. The time-dependent potential in a spherical cell using matched asymptotic expansions. *J. Math. Biol.* 2: 277–300.

Peskoff, A., R. S. Eisenberg, and J. D. Cole. 1976. Matched asymptotic expansions of the Green's function for the electric potential in an infinite cylindrical cell. *SIAM J. Appl. Math.* 30:222–239.

Plonsey, R., and R. C. Barr. 1986. Effect of microscopic and macroscopic discontinuities on the response of cardiac tissue to defibrillating (stimulating) currents. *Med. Biol. Eng. Comput.* 24:130–136.

Quan, W., and T. J. Cohen. 1993. Field stimulation of single cardiac cell: the dependency of membrane excitation threshold on waveform shape and cellular refractoriness. *In* Proceedings of the 15th Annual International Conference of the IEEE Engineering in Medicine and Biology Society. A. Y. J. Szeto and R. M. Rangayyan, editors. Institute of Electrical and Electronics Engineers, Inc., Piscataway, NJ. 869–870.

Schwann, H. P. 1983. Biophysics of the interaction of electromagnetic energy with cells and membranes. *In* Biological Effects and Dosimetry of Nonionizing Radiation. M. Grandolfo, S. M. Michaelson, and A. Rindi, editors. Plenum Press, New York. 213–231.

Teissie, J., and T. Y. Tsong. 1981. Electric field induced transient pores in phospholipid bilayer vesicles. *Biochemistry.* 20:1548–1554.

Tung, L., and J-R. Borderies. 1992. Analysis of electric field stimulation of cardiac muscle cells. *Biophys. J.* 63:1–16.

Tung, L., N. Sliz, and M. R. Mulligan. 1991. Influence of electrical axis of stimulation on excitation of cardiac muscle cells. *Circ. Res.* 69:722–730.